The Astrophysical Journal, 677:1378–1384, 2008 April 20

CME EARTHWARD DIRECTION AS AN IMPORTANT GEOEFFECTIVENESS INDICATOR

R.-S. Kim, K.-S. Cho, K.-H. Kim, and Y.-D. Park
Korea Astronomy and Space Science Institute, Daejeon 305-348, Korea; rskim@kasi.re.kr

Y.-J. Moon
Kyunghee University, Yongin 446-701, Korea

Y. Yi
Department of Astronomy and Space Science, Chungnam National University, Daejeon 305-754, Korea

J. Lee, H. Wang, and H. Song
New Jersey Institute of Technology, Newark, NJ 07102

and

M. Dryer
National Oceanic and Atmospheric Administration, Boulder, CO 80303
Received 2007 August 27; accepted 2007 December 19

ABSTRACT

Frontside halo coronal mass ejections (CMEs) are generally considered as potential candidates for producing geomagnetic storms, but there was no definite way to predict whether they will hit the Earth or not. Recently Moon et al. suggested that the degree of CME asymmetries, as defined by the ratio of the shortest to the longest distances of the CME front measured from the solar center, be used as a parameter for predicting their geoeffectiveness. They called this quantity a direction parameter, D, as it suggests how much CME propagation is directed to Earth, and examined its forecasting capability using 12 fast halo CMEs. In this paper, we extend this test by using a much larger database (486 frontside halo CMEs from 1997 to 2003) and more robust statistical tools (contingency table and statistical parameters). We compared the forecast capability of this direction parameter to those of other CME parameters, such as location and speed. We found the following results: (1) The CMEs with large direction parameters ($D \geq 0.4$) are highly associated with geomagnetic storms. (2) If the direction parameter increases from 0.4 to 1.0, the geoeffective probability rises from 52% to 84%. (3) All CMEs associated with strong geomagnetic storms ($\mathrm{Dst} \leq -200$ nT) are found to have large direction parameters ($D \geq 0.6$). (4) CMEs causing strong geomagnetic storms ($\mathrm{Dst} \leq -100$ nT), in spite of their northward magnetic field, have large direction parameters ($D \geq 0.6$). (5) Forecasting capability improves when statistical parameters (e.g., "probability of detection—yes" and "critical success index") are employed, in comparison with the forecast solely based on the location and speed of CMEs. These results indicate that the CME direction parameter can be an important indicator for forecasting CME geoeffectiveness.

Subject headings: solar-terrestrial relations — Sun: coronal mass ejections (CMEs)

1. INTRODUCTION

Coronal mass ejections (CMEs), gigantic magnetized clouds of plasma from the Sun, are known as a major cause of space weather disturbances that can influence the performance and reliability of modern technological systems (Schwenn 2006). But only a small portion of the CMEs can trigger geomagnetic storms. That is, prediction of a geomagnetic storm, using all CMEs, frequently results in false alarms. Thus, proper criteria to select geoeffective CMEs that cause geomagnetic storms ($\mathrm{Dst} \leq -50$ nT) are required, and a prediction capability test would be meaningful.

Several CME parameters have been proposed to select geoeffective CMEs as follows. First, the frontside halo CMEs with large angular width more than 120°, which appear as expanding and circular brightening that surrounds the coronagraph occulting disk, are known to be geoeffective because they are directed toward the Earth (Webb 2002; Gopalswamy et al. 2007). Poomvises & Zhang (2007) found, from the study of solar and interplanetary sources of major geomagnetic storms ($\mathrm{Dst} \leq -100$ nT), that the main source of a major geomagnetic storm is a fast full halo CME. Second, CME location and speed are also important geoeffective parameters. Wang et al. (2002) found that 83% of the frontside halo CMEs that caused geomagnetic storms with $Kp \geq 5$ took place within ±30° of the central meridian and that their source locations are asymmetrical in longitude with the majority located on the west side of the central meridian. Srivastava & Venkatakrishnan (2004) showed that the CME speeds in the LASCO field of view were roughly correlated with the strength of geomagnetic storms and that a large percentage (62%) of the geoeffective CMEs are faster than 700 km s^{-1}. Several studies suggested that fast halo CMEs, which occurred close to solar center, are favorable candidates for strong geomagnetic storms (Venkatakrishnan & Ravindra 2003; Srivastava 2005). Third, the magnetic field orientation of a CME's source region was suggested as an important parameter of the geoeffective CME (Pevtsov & Canfield 2001). Kang et al. (2006) found that southward orientation of the magnetic field in the CME source region plays an important role in the production of geomagnetic storm by investigation of the source region's shapes (S or inverse S) of the X-ray sigmoids associated with 63 CMEs. For about 84% of the CMEs, their geoeffective consequences are consistent with their magnetic field orientations. Song et al. (2006) showed that 92% (12/13) of the CME source regions associated with the super storms ($\mathrm{Dst} \leq -200$ nT) have southward field orientations as determined by the potential field extrapolation from daily full-disk MDI magnetograms. Fourth, Moon et al. (2005) proposed a CME earthward direction parameter, D (defined in

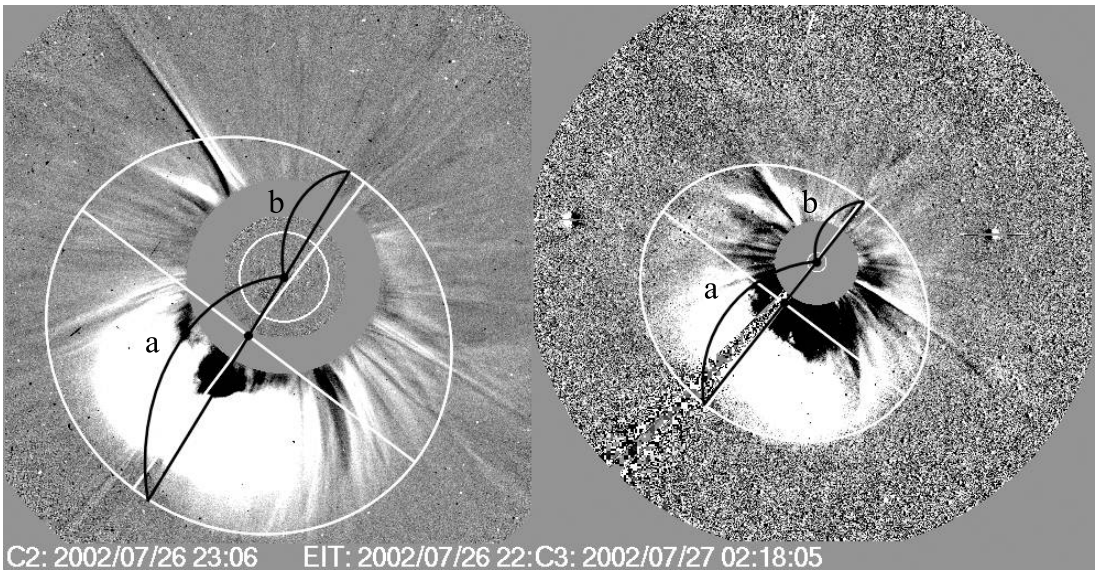

FIG. 1.— LASCO C2 (*left*) and C3 (*right*) images to illustrate how to estimate the direction parameter. The ratio of the shorter (*b*) to longer (*a*) distance of the CME front measured from the solar center along the line (*b*/*a*) is defined as the direction parameter, *D*. Note that the line passes both through the centers of the ellipse and the Sun.

§ 2.2), that quantifies the degree of asymmetry of the CME shape. They found, using 12 events, that the CME earthward direction seems to be the most important parameter in the geoeffectiveness of very fast halo CMEs ($\geq$1300 km s^{-1}).

One major concern faced by the space weather prediction challenge is to predict the arrival time of a CME at the Earth and the magnitude of the resulting geomagnetic storm. Several empirical and physics-based models have been proposed to predict the CME or CME-associated interplanetary (IP) shock arrival times based on their initial speeds. The IP shock, first to be examined, is the harbinger of a CME and can, itself, induce a sufficiently high dynamic pressure that can also be an important contributor to a geomagnetic storm (Gopalswamy et al. 2001; Zhang et al. 2003; Fry et al. 2003; Cho et al. 2003; McKenna-Lawlor et al. 2006; Kim et al. 2007). However, the forecast of geomagnetic storm strength and its probability, based on CME parameters, has not been widely investigated. Kim et al. (2005, hereafter Paper I) examined the relationship between CME parameters (location and speed) and Dst index as the geomagnetic storm strength and made forecast evaluations on the prediction of geoeffective CMEs using the contingency tables with individual parameters and their combination. They presented, for the first time, a probability map of geoeffective CMEs that depends on their source location and speed. It was found that the most probable source locations of halo CMEs to produce geomagnetic storms are $0^\circ < L < 30^\circ$ for slow ($<$800 km s^{-1}) CMEs and $-30^\circ < L < 60^\circ$ for fast ($\geq$800 km s^{-1}) CMEs, where L is the heliocentric longitude.

In this study we extend the work presented in Paper I by including the earthward direction parameter as another important factor. We reinvestigate the result of Moon et al. (2005) with a contingency table and probability map of geoeffective CMEs, from which we hope to be able to determine the most appropriate CME criteria for geoeffectiveness that are valid for a wider range of halo CMEs. This study also includes the forecast evaluation of geomagnetic storms by using CME parameters.

In § 2, we define the CME's earthward direction and explain how to determine the direction parameter, *D*. In § 3, we provide our results and discussion regarding the prediction probabilities of geoeffective CMEs, comparisons with other CME parameters, and a forecast evaluation based on a contingency table. A summary of our main results and conclusion are delivered in § 4.

2. METHODOLOGY AND DATA

2.1. *Data*

To examine the CME geoeffectiveness depending on its earthward direction parameter, we first considered 7742 CMEs observed by *SOHO* LASCO (Large Angle Spectroscopic Coronagraph; Brueckner et al. 1995) from 1997 to 2003. Since the measured CME properties such as linear plane-of-sky speeds, angular widths, and position angles are well compiled in the CME online catalog[1] (Yashiro et al. 2004), we easily selected 883 halo or partial halo CMEs whose angular width is equal to or larger than 120°. To select frontside halo CMEs we carefully compared the *SOHO* LASCO images with *SOHO* EIT running difference images. By investigating spatial and temporal closeness between the CME position and EUV features such as brightening or flare-associated ejecting loops, we selected 510 frontside halo CMEs.

The identification of geoeffective CMEs is done as follows. First, we estimated the arrival times of the selected 510 CMEs at the Earth by using the empirical CME propagation model (Gopalswamy et al. 2001). Second, we decided whether or not the CME is geoeffective by searching for the lowest value of Dst index from the National Space Science Data Center (NSSDC)[2] within a $\pm$24 hr time window from the predicted CME arrival time. According to Gonzalez et al. (1994), we defined the geomagnetic storms when the Dst index is below -50 nT or less. A detailed explanation on the selection procedure of the CME-Dst pairs can be found in Paper I. We confirmed that our CME-Dst pair identifications are mostly similar to those in other CME-Dst lists (Cane & Richardson 2003; Cho et al. 2003; Kang et al. 2006; Moon et al. 2005; Song et al. 2006; Zhang et al. 2003).

2.2. *Earthward Direction Parameter*

Even if we know the source location of a CME, we cannot assume the propagation direction, since all CMEs do not eject radially from the source region. In this respect, the direction parameter could be used to trace the CME's propagating direction at least near the Sun. If a CME is directly propagating toward the

[1] See http://cdaw.gsfc.nasa.gov/CME_list/index.html.
[2] See http://nssdc.gsfc.nasa.gov/omniweb/ow.html.

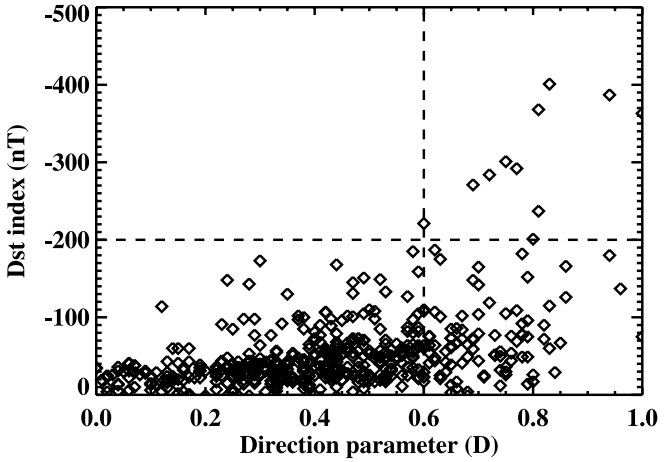

FIG. 2.—Direction parameter vs. Dst index for 486 frontside halo CMEs. The horizontal dashed line represents Dst = −200 nT, and the vertical dashed line indicates $D = 0.6$.

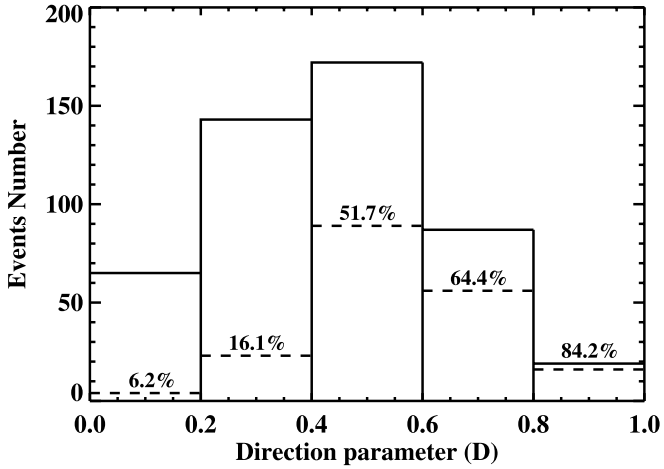

FIG. 3.—Number of events as a function of direction parameter. The dashed lines indicate the numbers of the geoeffective CMEs that caused the geomagnetic storm (Dst ≤ −50 nT) for given direction ranges, and the number on the dashed line means the probability of geoeffective CMEs. There is a general tendency that the probability of geoeffective CMEs increases with the direction parameter.

Earth, the shape of the CME front edge should be nearly symmetric, and the CME may trigger a geomagnetic storm. Otherwise, the shape should be quite asymmetric and the CME may not drive a geomagnetic storm. We thus define the direction parameter, D, as the ratio of distance between the shorter CME front and the solar center to that of the longer CME front; thus, it is always between 0 and 1.

The earthward direction parameter can be determined directly from a coronagraph observation. The measurement of the direction parameter is made as follows: (1) an ellipse is plotted to follow the CME front in the *SOHO* LASCO running difference image as shown in Figure 1; (2) we then draw a line that passes through the centers of both the Sun and the ellipse formed by the CME front; (3) we measure the ratio (b/a) of the shorter (b) to longer (a) distance of the CME front from the solar center along this line, and set the ratio as the direction parameter, D. Among 510 events, 24 events are so faint or multiple that we excluded these events (24/510, 4.7%). Since the direction parameter is applicable to most of the halo CMEs, the number of events (486) that we consider in this study is much more than that (305) of Paper I, in which the CMEs whose source locations were not available were excluded.

As illustrated in Figure 1, we measure the direction parameters for a single CME in LASCO C2 (*left*) and C3 (*right*) field of view. When we compare the direction parameters from both images, these two measured values are very similar to each other: 0.48 for C2 and 0.41 for C3. For all 486 events, the mean absolute difference from LASCO C2 and C3 is about 0.14. This fact implies that the CME earthward direction does not change much as the CME propagates. We use the direction parameters from LASCO C3 images, since they have clearer CME front edges than those from C2 images, and they give us final information on the CME propagation.

3. RESULTS AND DISCUSSION

3.1. *Relationship between Direction Parameter and Dst Index*

We examined the relationship between the CME direction parameter and the Dst index for 486 frontside halo CMEs. As a result, we found that 188 CMEs are geoeffective according to the criterion that they produced geomagnetic storms stronger than −50 nT (188/486, 40%). This result is very similar to that of Paper I. Figure 2 shows the distribution of the Dst index according to direction parameter. It is found that all CMEs associated with strong geomagnetic storms (Dst ≤ −200 nT) have large direction parameters ($D \geq 0.6$), as indicated by the dashed lines.

In order to gain an idea about achieving a criterion of the direction parameter for geoeffective CMEs we plot the probability of geoeffective CMEs as a function of their direction parameters in Figure 3. The dashed lines indicate the numbers of the geoeffective CMEs for given direction ranges. There is a general tendency that the probability of the geoeffective CMEs increases with the direction parameter. We note that the probabilities with a direction parameter larger than 0.4 are significantly higher than those with less direction parameter. In addition, it is found that the probability of a large direction parameter above 0.8 is about 84%, which is about 2 times higher than the mean probability. Since the probabilities are higher than the mean probability (40%) when the direction parameters are larger than 0.4, we can choose 0.4 as a criterion of direction parameter to predict geoeffective CMEs.

3.2. *Comparisons between Direction Parameter and Other Parameters*

Figure 4 shows the comparison between the direction parameter and the longitude of a source region for 287 CMEs whose

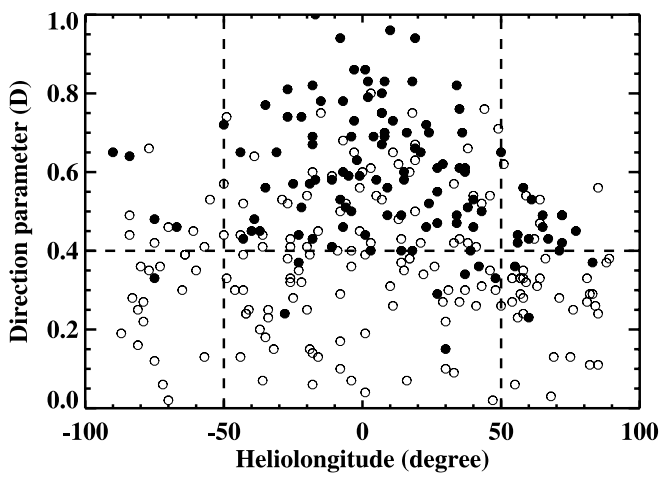

FIG. 4.—Heliolongitude vs. direction parameter for 287 frontside halo CMEs. The filled circles represent 115 geoeffective CMEs, and the empty circles, nongeoeffective events.

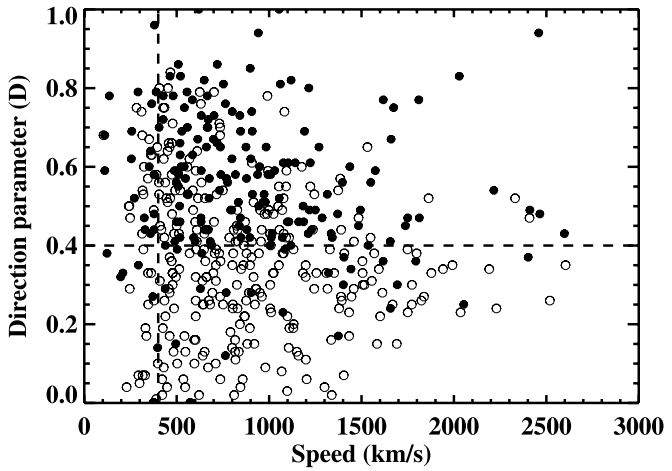

FIG. 5.—Plane-of-sky speed vs. direction parameter for 486 frontside halo CMEs. The filled circles represent 188 geoeffective CMEs, and the open circles, nongeoffective events.

locations were identified in Paper I and selected from all 486 CMEs. While the direction parameters are highly scattered for a given heliolongitude, there are few events that occurred near the limb but have a large direction parameter. If we consider the direction criterion as represented by the horizontal dashed line ($D = 0.4$) in Figure 4, it is found that 90% (104/115) of the geoeffective CMEs have larger direction parameters than the criterion. As compared with the location, 83% (95/115) of the geoeffective CMEs occurred in the location criterion ($L \leq |50^{\circ}|$) that was suggested in Paper I, as represented by two vertical dashed lines in the figure. A more detailed comparison in terms of a statistical forecast is described in § 3.3.

Figure 5 shows the comparison between the direction parameter and plane-of-sky speed for 486 frontside halo CMEs. There is a trend that very fast CMEs ($\geq$2000 km s^{-1}) have relatively small direction parameters near 0.4; that is, there are few very fast CMEs that have larger direction parameters than 0.6 or smaller direction parameters than 0.2. Noting that the speed is a plane-of-sky speed estimated from the LASCO images, it is likely that the speeds of the CMEs with large direction parameters would be affected more by the projection effect and, consequently, underestimated.

It is found that 86% (161/188) of the geoeffective CMEs have direction parameters larger than the value ($D = 0.4$) indicated by the horizontal dashed line in Figure 5. Also, 87% (164/188) of the geoeffective CMEs are faster than the speed criterion (400 km s^{-1}) indicated by the vertical dashed line that was proposed by Paper I. That paper also showed that the CME speed may be one of the criteria on which we might select a geoeffective CME, but it does not seem to be critical, since it produces many false alarms.

3.3. *Forecast Evaluation with Direction Parameter*

To our knowledge Paper I was the first forecast evaluation of the geoeffective CMEs to use the contingency tables and, thereby, to suggest the most reliable criteria: CME location ($L \leq 50^{\circ}$) and speed ($V \geq 400$ km s^{-1}). We evaluate the forecast capability of the direction parameter by using the contingency table and compare it with those from Paper I. The contingency table is widely used in the meteorological forecasting literature; it provides us with the information about the success or failure (or degree thereof) of the forecasting experience. Smith et al. (2000) first used the contingency table in the space weather context for predicting interplanetary shock times of arrival at Earth. In this study, we use several statistical parameters for forecast evaluation. The probability of detection—yes (PODy) means the proportion of yes observations that were correctly forecast, and the probability of detection—no (PODn) is the proportion of no observations that were correctly forecast. The false alarm ratio (FAR) is the proportion of yes predictions that were incorrect, and the bias is the ratio of yes predictions to yes observations. The critical success index (CSI) is the successful rate defined as the proportion of hits that were either predicted or observed. We also calculate some skill scores to compare with those from the forecasts by location and speed. True skill statistic (TSS) is a measure of the ability of the forecast to discriminate between yes and no observation. Heidke skill score (HSS) is the percent correct (hit or correct null) adjusted by the number expected to be correct by chance, and the Gilbert skill score (GSS) is the CSI corrected by the number of hits expected by chance. The general form of the contingency table and its statistical parameters can be found in Smith et al. (2000) and Paper I.

TABLE 1
CONTINGENCY TABLE BASED ON THE DIRECTION PARAMETER ($D \geq 0.4$)

	Observation		
Prediction	Yes	No	Total
Yes	161	117	278
No	27	181	208
Total	188	298	486

The criterion of direction parameter for geoeffective CMEs is determined as $D = 0.4$, which gives us the best result of forecast statistical parameters (practically the highest CSI). This estimate is consistent with the value determined from the fraction of geoeffective CMEs in Figure 3. In Table 1 the yes prediction is defined when the CME direction parameter is equal to or larger than 0.4. The yes observation indicates the occurrence of the geomagnetic storms (Dst ≤ -50 nT). Among 486 CMEs, 278 CMEs are classified to be yes predictions and 188 CMEs are found to be yes observations. Each value in this 2×2 table represents success or failure of the forecasting experience such as hits (161), false alarms (117), misses (27), and correct nulls (181).

Statistical parameters of forecast evaluation for the direction parameter are given in Table 2. The estimated PODy, PODn, FAR, bias, and CSI are 0.86, 0.61, 0.42, 1.48, and 0.53, respectively. Note that the better forecasts are indicated by statistical values that are closer to 1.0, except for FAR, which should be closer to 0.0 for a good forecast. As shown in Table 2, we also compare the results with those of the source location and the speed from Paper I. Even though the sample sizes are different (305 events in Paper I), it is found that most of the statistical parameters of the direction parameter are significantly better than those of the other

TABLE 2
COMPARISON OF THE FORECASTING STATISTICAL PARAMETERS

Parameter	Direction	Location	Speed
Probability of detection–yes (PODy)	0.86	0.79	0.91
Probability of detection–no (PODn)	0.61	0.36	0.11
False alarm ratio (FAR)	0.42	0.55	0.60
Bias	1.48	1.76	2.26
Critical success index (CSI)	0.53	0.40	0.39
True skill statistics (TSS)	0.47	0.15	0.02
Heidke skill score (HSS)	0.43	0.14	0.02
Gilbert skill score (GSS)	0.27	0.07	0.01

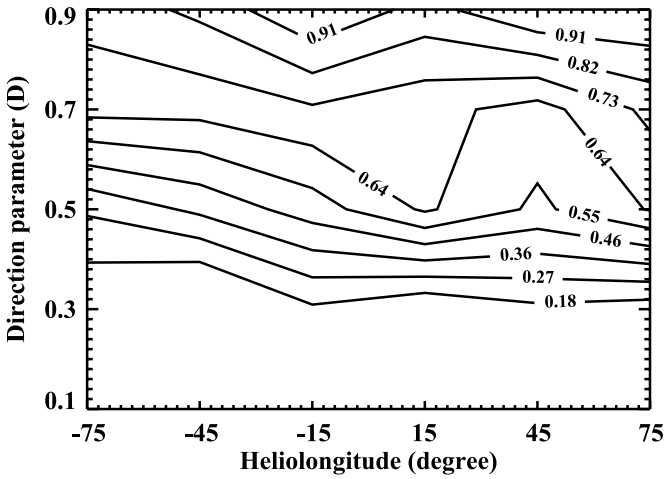

FIG. 6.— Probability map of goeffective CMEs depending on the combination of CME location and direction parameter.

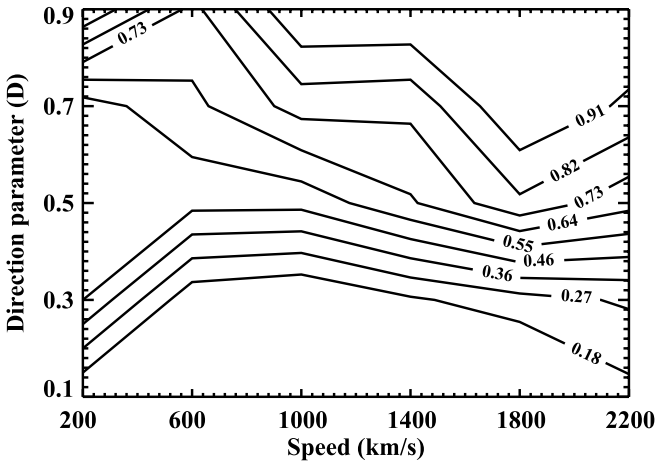

FIG. 7.— Probability map of geoeffective CMEs depending on the combination of CME speed and direction parameter.

parameters. In particular, CSI (0.53), which is used as an important index for forecast evaluation, is larger than that of CME location (0.40) and speed (0.39). Since TSS, HSS, and GSS are 0.47, 0.43, and 0.27, respectively, the skill scores for the direction parameter, D, are much better than those from location and speed.

3.4. *Probability Forecast*

We examined (Paper I) the probability of geoeffective CMEs depending on the combination of two parameters. We presented, in that work, a probability map of geoeffective CMEs depending on the combination of CME speed and location. This kind of work might help us to forecast the occurrence of geoeffective CMEs by taking probability considerations into account. We now extend this approach to consider the direction parameter, D. Figure 6 is the probability map of geoeffective CMEs depending on direction parameter and location for 287 events. The probability for an individual CME can, therefore, be forecasted according to its direction parameter and location from Table 3. We find a tendency that CMEs from disk center or western ($-30^\circ < L \leq 90^\circ$) events with large direction parameters are more geoeffective. For eastern ($-90^\circ < L \leq -30^\circ$) events the probabilities are higher than mean probability (40%) when their direction parameters are larger than 0.6. For disk center or western events, the probabilities are higher than the mean probability when their direction parameters are larger than 0.4. Note that some probabilities with small event numbers are regarded to be meaningless.

The probability of geoeffective CMEs depending on the combination of direction parameter and speed for 486 events is given in Figure 7 and Table 4. Even fast CMEs tend to be nongeoeffective when they have small direction parameters. The fast and earthward (i.e., large direction parameter) CMEs are more geoeffective than slow CMEs with small direction parameters. As shown in Figure 7, the direction parameter of the equiprobability line of 0.55 (55%) is above $D = 0.7$ when the speed is about 400 km s^{-1}, but it decreases to about $D = 0.4$ when the speed is faster than 2000 km s^{-1}.

3.5. *Usefulness of Direction Parameter for Northward Field Storm Events*

It is generally considered that geomagnetic storms are triggered by southward interplanetary magnetic fields (IMFs). Magnetic reconnections between southward IMF and the northward directed geomagnetic field occur at the day side magnetopause and then transport energy from the solar wind into the magnetosphere (Dungey 1961). If we assume that the field orientation of a CME is preserved during its interplanetary transit to Earth, we can expect that a CME with southward field orientation will cause a geomagnetic storm.

Recently, Song et al. (2006) investigated the relationship between magnetic structures of CME source regions and geomagnetic storms for 73 events. They defined the magnetic field orientation angle θ as the angle between the projection of the overlying potential field line on the solar surface and the direction toward the south pole. If $|\theta|$ is less than 90°, the magnetic field orientation of the CME is southward; otherwise it is northward. They showed that 73% (22/30) of the CME source regions associated with the strong geomagnetic storms (Dst ≤ -100 nT) had southward field orientations. These workers also noted that eight strong geomagnetic storms were caused by northward magnetic field CMEs.

In this respect, we feel that it is necessary to investigate the direction parameters for these exceptional events. From the list of 73 halo CMEs whose field orientations were estimated by

TABLE 3
PROBABILITY FORECAST OF FRONTSIDE HALO CMES BASED ON THEIR DIRECTION PARAMETER AND LOCATION FOR THE 287 EVENTS

DIRECTION PARAMETER	FRONTSIDE HALO CMES AT HELIOLONGITUDE (deg)						TOTAL
	$-90 \leq L \leq -60$	$-60 < L \leq -30$	$-30 < L \leq 0$	$0 < L \leq 30$	$30 < L \leq 60$	$60 < L \leq 90$	
$0.8 \leq D \leq 1$	0% (0/0)	0% (0/0)	100% (5/5)	88% (7/8)	100% (1/1)	0% (0/0)	93% (13/14)
$0.6 \leq D < 0.8$	67% (2/3)	67% (4/6)	71% (10/14)	67% (16/24)	60% (6/10)	0% (0/0)	67% (38/57)
$0.4 \leq D < 0.6$	29% (2/7)	38% (5/13)	50% (14/28)	65% (13/20)	53% (10/19)	64% (9/14)	52% (53/101)
$0.2 \leq D < 0.4$	9% (1/11)	0% (0/11)	17% (2/12)	9% (1/11)	16% (4/25)	13% (2/15)	12% (10/85)
$0 \leq D < 0.2$	0% (0/5)	0% (0/5)	0% (0/7)	0% (0/3)	20% (1/5)	0% (0/5)	3% (1/30)
Total	19% (5/26)	26% (9/35)	47% (31/66)	56% (37/66)	37% (22/60)	32% (11/34)	40% (115/287)

TABLE 4
PROBABILITY FORECAST OF FRONTSIDE HALO CMES BASED ON THEIR DIRECTION PARAMETER AND SPEED FOR THE 486 EVENTS

DIRECTION PARAMETER	FRONTSIDE HALO CMES AT SPEED (km s^{-1})						TOTAL
	$V < 400$	$V < 800$	$V < 1200$	$V < 1600$	$V < 2000$	$V \geq 2000$	
$0.8 \leq D \leq 1$	100% (1/1)	70% (7/10)	100% (5/5)	100% (1/1)	0% (0/0)	100% (2/2)	84% (16/19)
$0.6 \leq D < 0.8$	50% (9/18)	61% (27/44)	76% (13/17)	75% (3/4)	100% (4/4)	0% (0/0)	64% (56/87)
$0.4 \leq D < 0.6$	47% (8/17)	48% (30/62)	48% (28/58)	63% (15/24)	80% (4/5)	67% (4/6)	52% (89/172)
$0.2 \leq D < 0.4$	45% (5/11)	11% (5/44)	8% (3/40)	17% (4/24)	24% (4/17)	29% (2/7)	16% (23/143)
$0 \leq D < 0.2$	9% (1/11)	8% (2/25)	0% (0/20)	13% (1/8)	0% (0/1)	0% (0/0)	6% (4/65)
Total	41% (24/58)	38% (71/185)	35% (49/140)	39% (24/61)	44% (12/27)	53% (8/15)	39% (188/486)

Song et al. (2006), we select 64 CMEs whose direction parameters are well determined. Figure 8 shows the magnetic field orientation angle, θ, versus the Dst index for the CMEs. We found that about 75% (30/40) of geoeffective CMEs (Dst ≤ -50 nT) have southward magnetic field orientations ($|\theta| < 90^\circ$). We note six exceptional events that have northward magnetic field orientations but, nevertheless, caused strong geomagnetic storms ($D \leq -100$ nT). Figure 9 shows the direction parameter versus the Dst index for 23 northward CMEs among 64 events. It is very interesting to note that all six exceptional events have large direction parameters ($D \geq 0.6$).

4. SUMMARY AND CONCLUSION

We have examined the geoeffectiveness of frontside halo CMEs and its dependence on CME physical parameters, especially the CME earthward direction parameter. This parameter ($D = b/a$, as defined in Fig. 1) indicates the degree of asymmetry of the CME front and can be a proxy to represent the CME propagation to the Earth. In this paper we investigated in detail whether the direction parameter is valid for selecting geoeffective CMEs and compared its capability with those of other parameters (source location and speed). For this purpose, we made their forecast evaluations using contingency tables; we also presented probability maps of geoeffective CMEs. Our main results can be summarized as follows.

1. The mean probability of geoeffective CMEs associated with geomagnetic storms (Dst ≤ -50 nT) is about 40% (188/486). The storm strength for a given direction parameter is relatively well correlated with an associated CME's direction parameter, and all CMEs associated with strong geomagnetic storms (Dst ≤ -200 nT) have direction parameters larger than 0.6.

2. CMEs with large direction parameters ($D \geq 0.4$) are highly associated with geomagnetic storms, and their association probability rises from 52% to 84% as the direction parameter increases from 0.4 to 1.0.

3. The forecast evaluation with contingency tables shows that most of the statistical parameters and skill scores of the direction parameter are much better than those that refer to location and speed. In particular, CSI (0.53), which is used as an important index for forecast evaluation, is much larger than that of CME location (0.40) and speed (0.39).

4. We present probability maps depending on the combinations of direction parameter and location, as well as direction parameter and speed. It is found that the disk or western CMEs ($-30^\circ < L \leq 90^\circ$) with large direction parameters are more geoeffective. The probability of a geoeffective CME increases with direction parameter and speed and is much more sensitive to the former than the latter. These probability maps can be directly used for practical forecasts of geomagnetic storms based on frontside halo CME data.

5. Using magnetic field orientation data of 64 CMEs from Song et al. (2006), we examined their direction parameters and CME geoeffectiveness. As a result, we found that all six northward CMEs that produced strong geomagnetic storms ($D \leq -100$ nT) have large direction parameters ($D \geq 0.6$). We speculate that these

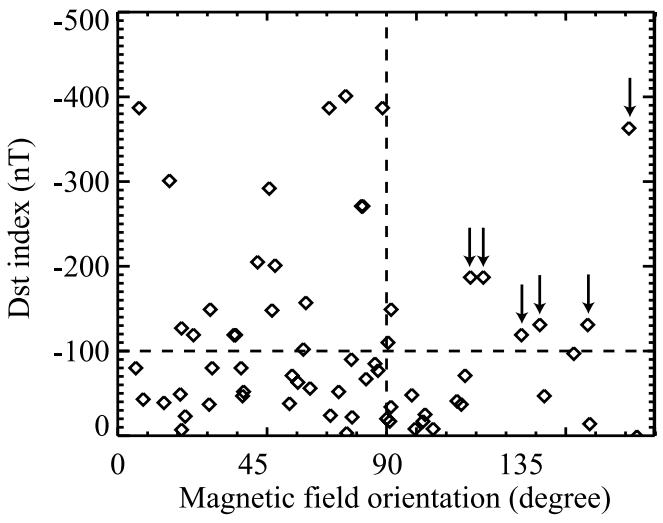

FIG. 8.—Magnetic field orientation angle vs. Dst index for 64 CMEs that Song et al. (2006) analyzed. The arrows indicate six exceptional events that have northward magnetic field orientation but produced strong geomagnetic storms (Dst ≤ -100 nT).

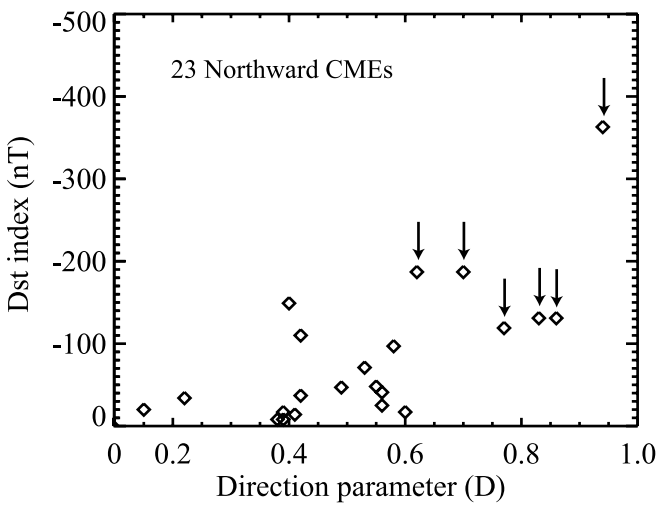

FIG. 9.—Direction parameter vs. Dst index for 23 northward CMEs among the 64 events studied by Song et al. (2006). It is clear that all six exceptional events indicated by arrows have large direction parameters ($D \geq 0.6$).

six CMEs possessed shock waves with associated high dynamic pressure impacts on the bow shock–magnetosphere system.

Our results confirm that the direction parameter is superior to source location and speed for selecting geoeffective CMEs. It is valuable not only for fast CMEs but also for all frontside halo CMEs. In addition, the direction parameter can be determined directly from coronagraph observations so that it is applicable to most of the halo CMEs, even though the frontside CME may have an unknown source region. Among 510 frontside halo CMEs, while we determined the locations of only 305 CMEs (about 60%), we estimated the direction parameters of 486 CMEs (about 95%). This point is very important for practical forecasts. Thus, we conclude that the direction parameter is useful for forecasting geoeffective CMEs. Physical interpretation of the direction parameter may be revealed if empirical three-dimensional (3D) mapping of CMEs from *STEREO* data may become available in the near feature. Physics-based modeling of ICMEs (CMEs and their interplanetary shocks) has already been started (Intriligator et al. 2006, 2007; Wu et al. 2007a, 2007b; Sun et al. 2007) as reviewed by Dryer (2007).

The present work, together with our previous paper (Kim et al. 2005), shows a sufficient possibility to forecast geomagnetic storms using frontside halo CMEs. Of course, we have to consider the IP shocks and the real-time conditions of near Earth for more accurate forecasts (Dryer 1998); however, forecasts using only CME parameters would be very meaningful in that they would allow us to make an earlier warning of specific Dst minimum levels of geomagnetic storms 2–3 days in advance.

This work was supported by a Korea Research Foundation grant funded by the Korean Government (MOEHRD; KRF-2006-612-C00014) and by the Development of Korean Space Weather Center, a project of KASI, and the KASI basic research fund. The CNU group was supported by the grant (F01-2003-000-00186-0) from the Korea Science and Engineering Foundation (KOSEF). J. L. was supported by NSF grant AST 06-07544 and NASA grant NNG0-6GE76G. M. D. was supported by NASA's Living with a Star Program via grant NAG5-12527 to Exploration Physics International, Inc. M. D. also thanks NOAA's Space Weather Prediction Center for their hospitality during his emeritus status. The CME catalog used here is generated and maintained by NASA and the Catholic University of America in cooperation with the Naval Research Laboratory. *SOHO* is a project of international cooperation between ESA and NASA. The Dst index is provided by the World Data Center for Geomagnetism at Kyoto University.

REFERENCES

Brueckner, G. E., et al. 1995, Sol. Phys., 162, 357
Cane, H. V., & Richardson, I. G. 2003, J. Geophys. Res., 108, 1156
Cho, K.-S., Moon, Y.-J., Dryer, M. , Fry, C. D. , Park, Y.-D., & Kim, K.-S. 2003, J. Geophys. Res., 108, 1445
Dryer, M. 1998, AIAA J., 36, 365
———. 2007, Asia J. Phys., 16, 97
Dungey, J. W. 1961, Phys. Rev. Lett., 6, 47
Fry, C. D., Dryer, M., Smith, Z., Sun, W., Deehr, C. S., & Akasofu, S.-I. 2003, J. Geophys. Res., 108, 1070
Gonzalez, W. D., Joselyn, J. A., Kamide, Y., Kroehl, H. W., Rostoker, G., Tsurutani, B. T., & Vasyliunas, V. M. 1994, J. Geophys. Res., 99, 5771
Gopalswamy, N., Lara, A., Yashiro, S., Kaiser, M. L., & Howard, R. A. 2001, J. Geophys. Res., 106, 29207
Gopalswamy, N., Yashiro, S., & Akiyama, S. 2007, J. Geophys. Res., 112, A06112, DOI: 10.1029/2006JA012149
Intriligator, D. S., Rees, A., Horbury, T., Sun, W., Detman, T., Dryer, M., Deehr, C., & Intriligator, J. 2007, in Proc. 6th IGPP Int. Astrophys. Conf. (New York: AIP), 932, 167
Intriligator, D. S., Sun, W., Detman, T., Dryer, M., Fry, C. D., Deehr, C., & Intriligator, J. 2006, in Proc. 5th IGPP Int. Astrophys. Conf., Physics of the Inner Heliosheath: Voyager Observations, Theory, and Future Prospects, ed. J. Heerikhuisen et al. (New York: AIP), 64
Kang, S.-M., Moon, Y.-J. , Cho, K.-S., Kim, Y.-H., Park, Y. D., Baek, J.-H., & Chang, H.-Y. 2006, J. Geophys. Res., 111, A05102, DOI: 10.1029/2005JA011445
Kim, K.-H., Moon, Y.-J., & Cho, K.-S. 2007, J. Geophys. Res., 112, A05104, DOI: 10.1029/2006JA011904
Kim, R.-S., Cho, K.-S., Moon, Y.-J., Kim, Y.-H., Yi, Y., Dryer, M., Bong, S.-C., & Park, Y.-D. 2005, J. Geophys. Res., 110, A11104, DOI: 10.1029/2005JA011218 (Paper I)
McKenna-Lawlor, S. M. P., Dryer, M., Kartalev, M. D., Smith, Z., Fry, C. D., Sun, W., Deehr, C. S., Kecskemety, K., & Kudela, K. 2006, J. Geophys. Res., 111, A11103, DOI: 10.1029/2005JA011162
Moon, Y.-J., Cho, K.-S., Dryer, M., Kim, Y.-H., Bong, S.-C., Chae, J., & Park, Y. D. 2005, ApJ, 624, 414
Pevtsov, A., & Canfield, R. C. 2001, J. Geophys. Res., 106, 25191
Poomvises, W., & Zhang, J. 2007, AAS Meeting, 210, 30.07
Schwenn, R. 2006, Living Rev. Sol. Phys., 3, 2
Smith, Z., Dryer, M., Ort, E., & Murtagh, W. 2000, J. Atmos. Solar-Terr. Phys., 62, 1265
Song, H., Yurchyshyn, V., Yang, G., Tan, C., Chen, W., & Wang, H. 2006, Sol. Phys., 238, 141
Srivastava, N. 2005, Ann. Geophys., 23, 2989
Srivastava, N., & Venkatakrishnan, P. 2004, J. Geophys. Res., 109, A10103, DOI: 10.1029/2003JA010175
Sun, W., Deehr, C. S., Fry, C. D., Dryer, M., Smith, Z., & Akasofu, S.-I. 2007, Space Weather, in press
Venkatakrishnan, P., & Ravindra, B. 2003, Geophys. Res. Lett., 30, 2181, DOI: 10.1029/2003GL018100
Wang, Y. M., Ye, P. Z., Wang, S., Zhau, G. P., & Wang, J. 2002, J. Geophys. Res., 107, 1340, DOI: 10.1029/2002JA009244
Webb, D. F. 2002, in Proc. *SOHO*-11 Symp., From Solar Min to Max: Half a Solar Cycle with *SOHO*, ed. A. Wilson (ESA SP-508; Noordwijk: ESA), 409
Wu, C.-C., Fry, C. D., Dryer, M., Wu, S. T., Thompson, B., Liou, K., & Feng, X. S. 2007a, J. Adv. Space Res., 40, 1827, DOI: 10.1016/j.asr.2007.06.025
Wu, C.-C., Fry, C. D., Wu, S. T., Dryer, M. & Liou, K. 2007b, J. Geophys. Res., 112, A09104, DOI: 10.1029/2006JA012211
Yashiro, S., Gopalswamy, N., Michalek, G., St. Cyr, O. C., Plunckett, S. P., & Howard, R. A. 2004, J. Geophys. Res., 109, A07105, DOI: 10.1029/2003JA010282
Zhang, J., Dere, K. P., Howard, R. A., & Bothmer, V. 2003, ApJ, 582, 520